Gain spectra of beam coupling in photorefractive semiconductors

G. Brost

Air Force Research Laboratory, 25 Electronic Parkway, Rome, New York 13441

J. Norman*

Department of Physics and Astronomy, Vassar College, Poughkeepsie, New York 12604

S. Odoulov, K. Shcherbin, A. Shumelyuk, and V. Taranov

Department of Quantum Electronics, Institute of Physics of National Academy of Sciences of Ukraine, Kiev, 252 650 UA, Ukraine

Received August 29, 1997

The photorefractive recording dynamics of two-beam coupling in semi-insulating semiconductors by beams with slightly different frequencies are studied theoretically and experimentally. The influences of bulk absorption, Gaussian beam profiles, and experimental geometry on the temporal response are analyzed. These effects act to narrow the bandwidth. Measurement of the material photorefractive time constant is discussed.
 [S0740-3224(98)00307-5]
OCIS codes: 190.5330, 190.7070, 130.5990.

1. INTRODUCTION

Measurement of the temporal response of two-beam coupling in photorefractive materials is important for determination of material parameters and for device characterization. However, there are a number of experimental and material factors that can strongly influence such measurements. These factors include bulk absorption, beam intensity profiles, coupling geometry, coupling strength, modulation depth, dark current, and pump depletion. Even under conditions in which only absorption appears to be a factor, the bandwidth of the material can be drastically different from that predicted by the standard photorefractive theory.

In fast photorefractive materials, such as the II–VI and III–V semiconductors, it is often convenient to measure the temporal response in the frequency domain rather than in the time domain. This approach eliminates the requirement of fast shutters and detectors and has the advantage that measurements in the frequency domain are carried out entirely in the steady-state regime. In addition, for purposes of accounting for the influences on the temporal response mentioned above, working in the frequency domain is particularly convenient because modeling is often more readily done there.

In the diffusion regime the standard solution of the material equations for a material with one kind of photorefractive trap predicts that the time dependence of the gain coefficient is given by[1]

$$\Gamma = \Gamma_0[1 - \exp(-t/\tau)], \tag{1}$$

where Γ_0 is the steady-state gain coefficient and τ is the photorefractive time constant. In the frequency domain the two-beam coupling gain spectra for moving gratings are given by[2]

$$\Gamma = \Gamma_0/(1 + \Omega^2\tau^2), \tag{2}$$

where Ω is the angular frequency detuning between the pump and the signal beams. Equation (2) is a simple Lorentzian function centered at $\Omega = 0$ Hz. Derivation of Eqs. (1) and (2) assumes negligible contributions from the factors mentioned in the first paragraph. In particular, it assumes a lossless material and plane-wave illumination. In practice, these conditions cannot be met. The photorefractive response time is dependent on intensity and is therefore position dependent in the material.

The effect of absorption on the photorefractive response was investigated in Refs. 3–5. Dai *et al.*[3] and Delaye *et al.*[4] showed that the bandwidth of the response narrows for a lossy material. Hermanns *et al.*[5] derived the transfer function in the presence of absorption and the absence of pump depletion. The problem of two-beam coupling with focused Gaussian beams in planar waveguides was analyzed by Fluck *et al.*[6] In that case the interaction length was determined by the beam profile rather than by the thickness of the material. They found that the transverse intensity distribution of the Gaussian beams must be taken into account in evaluation of the gain and that the time response can differ from that predicted by plane-wave theory. Boutsikaris and Davidson[7] dealt with the problem of transient two-beam coupling with non-plane-wave beams in a lossless medium.

Part of the reason that the problem of two-beam coupling including simultaneous absorption and non-plane-wave beams had not been widely treated may be the fact that, in the absence of dark current or beam depletion ef-

fects, the steady-state gain is relatively insensitive to total intensity. The temporal response, in contrast, is highly sensitive to the volume distribution of the intensity in the material. Optical absorption and beam geometries both are important factors that influence the gain spectra of semiconductors. For a given input light intensity the optical absorption determines the upper limit of the bandwidth. For typical experimental configurations in bulk photorefractives, in which the beams are not strongly focused, the beam profiles do not strongly influence the steady-state, degenerate two-beam coupling gain, since the interaction length is determined by the material thickness. For focused or small-diameter beams, issues of beam depletion and dark intensity come into play, and the interaction length may be determined by the beam profiles themselves.[6]

In this paper we study the influence of a spatially dependent light-intensity distribution on the gain spectra of the photorefractive. It is assumed here that dark current, large modulation, and pump depletion are not present and that the gain is in the small-signal regime. We present a theoretical analysis that elucidates the effects of optical absorption and Gaussian beam profiles. We also present experimental results of gain spectra and temporal response measured in photorefractive semiconductors. We find that the frequency response can significantly depart from the Lorentzian shape of Eq. (2). We use a simple method of eliminating these influences for the purpose of measuring the material photorefractive time constant.

2. THEORY

A. Absorption

In this section we consider the effect of optical absorption on the gain spectra. We assume that the signal beam intensity is much smaller than the pump beam intensity and that the pump beam provides uniform illumination distribution in the transverse direction but falls off exponentially with distance according to Beer's law, $I(z) = I_0 \exp(-\alpha z)$. We also assume that the photorefractive response time is inversely proportional to some power q of the light intensity, so that the position-dependent response time is given by

$$\tau(z) = \tau_0[I_0/I(z)]^q = \tau_0 \exp(q\alpha z), \tag{3}$$

where τ_0 is the photorefractive time constant at intensity I_0, at the front of the crystal. The integral gain coefficient for moving gratings is then given by

$$\Gamma = \frac{1}{L}\int_0^L \frac{\Gamma_0}{1 + \Omega^2\tau^2(z)}\,dz, \tag{4}$$

where L is the interaction length. After substitution for $\tau(z)$ and integration the final expression for the gain spectrum becomes

$$\Gamma = \Gamma_0 = \left\{1 + \frac{1}{2q\alpha L}\ln\left[\frac{1 + \Omega^2\tau_0^2}{1 + \Omega^2\tau_0^2\exp(2q\alpha L)}\right]\right\}. \tag{5}$$

This result agrees with the transfer function derived by Hermanns *et al.*[5] for $q = 1$. Figure 1 demonstrates the

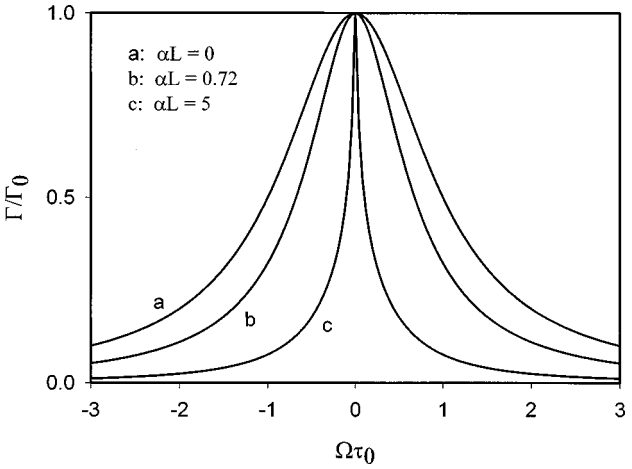

Fig. 1. Gain spectra for three values of αL.

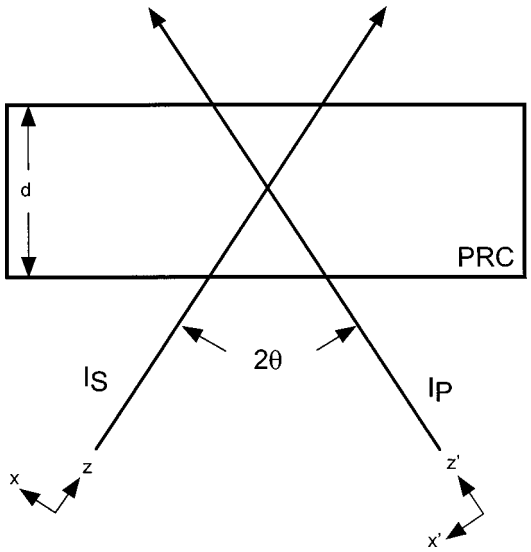

Fig. 2. Schematic of the beam coupling interaction: PRC, photorefractive crystal.

effect of absorption on the gain spectra. Here we plot the gain coefficient as a function of the normalized frequency detuning for three values of αL with $q = 1$: $\alpha L = 0$, $\alpha L = 0.72$, and $\alpha L = 5$. Curve a is the single Lorentzian profile given by Eq. (2) for no absorption. Curve b reflects an αL for typical crystal parameters. In this case the gain profile can still be characterized as single Lorentzian but narrower than for no absorption. This result shows that the effect of absorption for most crystals is to increase the exponential time constant, in this case by ~50%. Curve c demonstrates the effect of large absorption. In this case the gain profile is much narrower (by a factor of ~10) than in the no-absorption case. It can no longer be characterized as a single Lorentzian. In fact, it is more accurately described as the sum of two Lorentzians.

B. Gaussian Beam Profiles

We now consider the more general case of finite beam sizes. The geometry is as shown in Fig. 2. Signal beam I_S and pump beam I_P cross inside a crystal of thickness d

at an angle of 2θ. The intensity profiles of the signal and the pump beams are assumed to be Gaussian and are given by

$$I_S(x, y, z) = I_{S0} \exp\left[\frac{-2(x^2 + y^2)}{{\omega_S}^2}\right]\exp(-\alpha z), \quad (6)$$

$$I_S(x', y', z') = I_{S0} \exp\left[\frac{-2(x'^2 + y'^2)}{{\omega_P}^2}\right]\exp(-\alpha z'), \quad (7)$$

where $2\omega_S$ and $2\omega_P$ are the $1/e^2$ intensity diameters of the signal and the pump beams, respectively. As before, we assume that the pump beam intensity is much larger than the signal beam intensity, so $\tau(I)$ is determined by I_P. We calculate the gain coefficient by integrating the differential gain coefficient over the volume of the signal beam. After a coordinate transformation from the primed to the unprimed coordinates, and after we take the origin to be where the beams cross, the gain coefficient is given by

$$\Gamma = \frac{\Gamma_0 2\cos(\theta)}{\pi {\omega_S}^2 d} \int_{\frac{-\xi d}{\cos(\theta)}}^{\frac{(1-\xi)d}{\cos(\theta)}} \int_{-\infty}^{\infty}\int_{-\infty}^{\infty} \times \frac{\exp\left[\frac{-2(x^2 + y^2)}{{\omega_S}^2}\right] dy\, dx\, dz}{1 + \Omega^2 + {\tau_0}^2 \exp\left\{2q\alpha\left[-\sin(2\theta)x + \cos(2\theta)y + \frac{\zeta d}{\cos(\theta)}\right]\right\}\exp\left\{\frac{4[\cos(2\theta)x + \sin(2\theta)z]^2 + 4y^2}{{\omega_P}^2}\right\}}. \quad (8)$$

Here the differential gain is weighted according to the Gaussian profile of the signal beam, d is the crystal thickness, and ξ is a parameter that indicates the location of the origin. The integral given in Eq. (8) was evaluated numerically.

There are seven parameters that influence the gain coefficient in Eq. (8): q, α, d, ω_S, ω_P, θ, and ξ. It is not possible here to fully evaluate the effect of each parameter. We highlight some of the more important features. In the following analysis we let $q = 1$, $\alpha = 1.2\ \mathrm{cm}^{-1}$, $d = 0.6$ cm, and $2\omega_S = 2$ mm.

In Fig. 3 the calculated gain spectra are plotted for crossing angles of $2\theta = 0°$ and $2\theta = 25°$, with $2\omega_P = 2$ mm and the beams crossing in the center of the crystal ($\xi = 1/2$). The gain calculated from Eq. (5) for plane waves is also shown for comparison (curve a). The position-dependent intensity associated with the Gaussian beam profile causes a significant narrowing of the bandwidth compared with that of the plane-wave case, a factor of ~5 for $2\theta = 25°$. The resulting gain spectrum is similar to that of the plane-wave, large-absorption example in Fig. 1. Of course, the departure from Lorentzian shape is less pronounced for thin crystals.

The influence of the Gaussian beam profile can be minimized with an expanded pump beam. Figure 4 shows the calculated gain for a crossing angle of $2\theta = 25°$, $\xi = 1/2$, and $\omega_P = \omega_S, 2\omega_S, 5\omega_S$. There is still appreciable narrowing of the gain spectrum for $\omega_P = 2\omega_S$, but the spectrum is not much different from that in the plane-wave case for $\omega_P = 5\omega_S$.

In the previous examples the beams were assumed to cross at the center of the crystal. Figure 5 shows the calculated gain spectra for various crossing locations, $\xi = 0, 1/2, 1$, corresponding to the front, the center, and the back of the crystal, respectively, with $\omega_P = 3\omega_S$ and a crossing angle of $2\theta = 25°$. Although the steady-state gain in the degenerate case does not depend on ξ, the bandwidth does. The widest bandwidth is obtained when the beams cross at the center of the crystal.

C. Discussion

With a nonuniform intensity distribution the photorefractive time constant is position dependent. The measured response is then a superposition of the response at all points in the crystal volume that is occupied by the signal beam. As the frequency is increased, the slower parts of the crystal, corresponding to lower total light intensity, fall off first in gain. At high frequencies only the fast parts of the crystal have significant gain. The net result is a faster falloff of measured gain with frequency than is expected from the case of uniform intensity, that is, a narrowing of the system bandwidth. Whereas bulk absorption causes the gain near the exit face of the crystal to decrease with frequency more rapidly than at the entrance face, the Gaussian intensity profile of the pump beam causes the gain to decrease with frequency nonuniformly

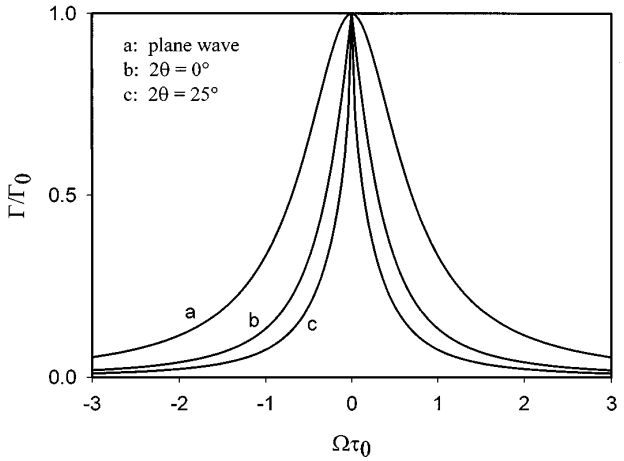

Fig. 3. Calculated gain spectra for different crossing angles. Parameters were $q = 1$, $\alpha = 1.2\ \mathrm{cm}^{-1}$, $d = 0.6$ cm, $2\omega_S = 2$ mm, $2\omega_P = 2$ mm, and $\xi = 1/2$.

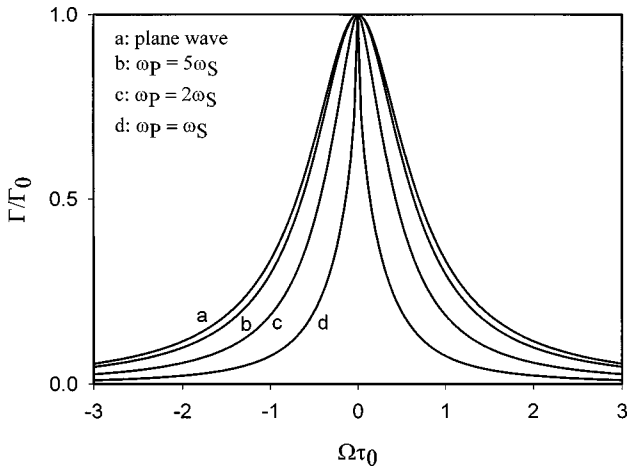

Fig. 4. Calculated gain spectra for several pump beam sizes. Parameters were $q = 1$, $\alpha = 1.2\ \mathrm{cm}^{-1}$, $d = 0.6$ cm, $2\omega_S = 2$ mm, $2\theta = 25°$, and $\xi = 1/2$.

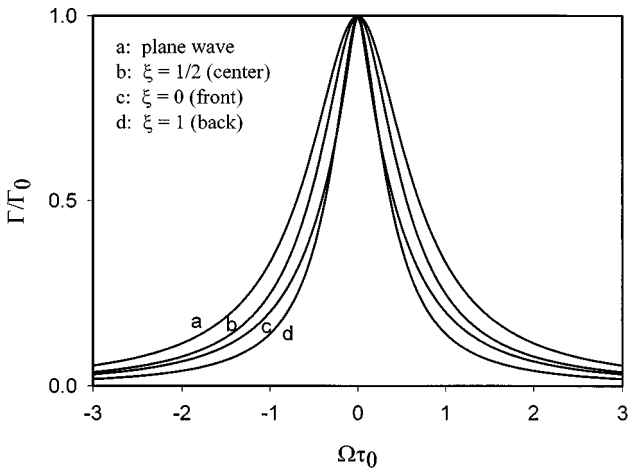

Fig. 5. Calculated gain spectra for three beam crossing locations. Parameters were $q = 1$, $\alpha = 1.2\ \mathrm{cm}^{-1}$, $d = 0.6$ cm, $2\omega_S = 2$ mm, $2\omega_P = 6$ mm, and $2\theta = 25°$.

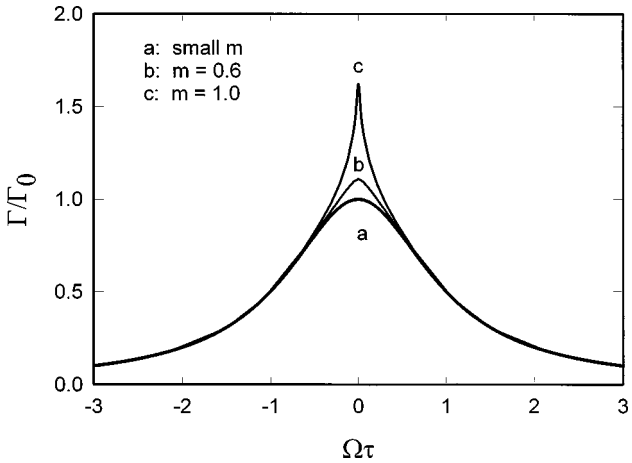

Fig. 6. Calculated gain spectra for three values of modulation m.

in a direction approximately transverse to the signal beam. The gain spectra given by Eq. (8) predict the photorefractive response in the presence of absorption and collimated Gaussian beams.

There are some limits on the applicability of Eq. (8). The main limitation concerns the assumption that the pump beam intensity is significantly greater than that of the signal beam. This applies not just to the peak intensities but throughout the volume of the signal beam. Equation (8) assumes that the time dependence is determined by the pump beam intensity alone and not by that of the signal beam. Also, this approach does not account for the effects of large modulation, beam depletion, or dark current that could occur in the Gaussian wings. Consequently, the limit of application depends on the geometry of the problem. The examples presented here are valid for beam ratios greater than 100. In the case of small beam diameters and thick crystals, the photorefractive interaction may occur far enough out in the wings of the pump beam that these assumptions are no longer valid. For these problems the numerical approach of Fluck *et al.*[6] is more appropriate. Also, note that the results presented here are limited to beam coupling. The diffraction efficiency spectra may be different. This is so because beam coupling gain is independent of modulation, while the diffraction efficiency is proportional to m^2. With Gaussian beams the modulation will be position dependent.

The present analysis did not consider the effects of beam coupling on the time constant. Analysis of the photorefractive response that included the interaction of the optical field with the space-charge field has shown a decreased bandwidth for materials with large ΓL, such as the ferroelectrics.[8,9] For semiconductors the gain is sufficiently small that this effect is negligible.

A non-Lorentzian gain spectrum can be obtained under certain experimental conditions, even when the pump beam diameter is much greater than the signal beam diameter. The nonlinearity of the photorefractive response is such that at large modulation the response becomes superlinear but with a slow temporal component.[10] A calculation of the gain spectra for various values of m is shown in Fig. 6. These results are solutions of the material equations and reflect the local response for plane waves. For $m < 0.6$ the response does not deviate much from the small-m result of Eq. (2). For larger values of m the space-charge field is enhanced, but only for small frequency shifts owing to the slow time component.

It should also be noted that deviations from the Lorentzian shape can occur for reasons related not to the experimental conditions but to the physics. For example, in $Sn_2P_2S_6$ (Ref. 11) a dip in the gain occurs near 0 Hz. This dip points to the presence of a second grating of opposite sign. Similar deviations could occur in other photorefractive crystals, including semiconductors, in which, for example, electron–hole competition is sometimes observed.

3. EXPERIMENTAL RESULTS

In this section we present measured two-beam coupling frequency and time response data. As predicted in Section 2, it is found that the temporal response varies considerably with changes in Gaussian beam sizes and coupling geometry and is influenced strongly by the bulk absorption of the material.

The experimental configuration for our measurements of two-beam coupling frequency and time response is shown in Fig. 7. The moving grating was produced in the photorefractive crystal by linear phase modulation of one of the beams with an electro-optic phase modulator. In the frequency-response measurements the steady-state gain was measured as a function of the frequency, $f = \Omega/2\pi$, of the ramp applied to the electro-optic modulator. The velocity of the grating is simply related to this frequency by $v_g = \Lambda f$, where Λ is the grating spatial period, because the ramp amplitude was adjusted for a 2π-phase excursion.

The two-beam coupling measurements were performed at a wavelength of 1.06 μm and a grating period of 0.7 μm. The laser beams were incident upon the $(1\bar{1}0)$ face of the GaAs:Cr crystal, the grating vector was oriented in the $\langle 001 \rangle$ direction, and the beams were s polarized, i.e., along the $\langle 110 \rangle$ direction, to take advantage of the r_{41} electro-optic coefficient. The dimensions of the crystal, in the directions $\langle 110 \rangle \times \langle 100 \rangle \times \langle 1\bar{1}0 \rangle$, were 11 mm $\times$ 10 mm $\times$ 6.1 mm, and the measured absorption coefficient was 1.2 cm^{-1}.

Our two-beam coupling frequency and time-response data for the GaAs:Cr sample, corresponding to various illumination conditions, are shown in Figs. 8–14 below. Next we describe the effects of these illumination conditions and of the material absorption on the temporal response of our sample.

In Fig. 8 the Gaussian signal and pump beams have $1/e^2$ diameters of 1.8 and 2.0 mm, respectively. The data of Figs. 8(a) and 8(b), corresponding to the frequency and the time response, respectively, were acquired under identical experimental conditions. Note that the beam diameters in this case are much smaller than the crystal thickness of 6.1 mm. The dashed curve in Fig. 8(a) is an attempt to fit the data to the Lorentzian of Eq. (2), and it is apparent that the data depart significantly from this model. If the assumptions inherent in Eq. (2) were valid, the material time constant would be related to the full width at half-maximum, Δ, of the Lorentzian by $\tau = 1/\pi\Delta$.

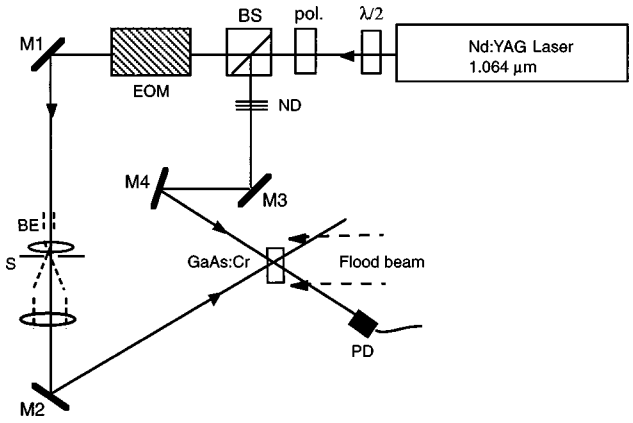

Fig. 7. Configuration for the measurement of frequency and time responses of two-beam coupling: M1–M4, mirrors; λ/2, half-wave plate; pol, linear polarizer; BS, beam splitter; EOM, electro-optic phase modulator; BE, variable beam expander; S, mechanical shutter; PD, photodetector; ND, neutral-density filters.

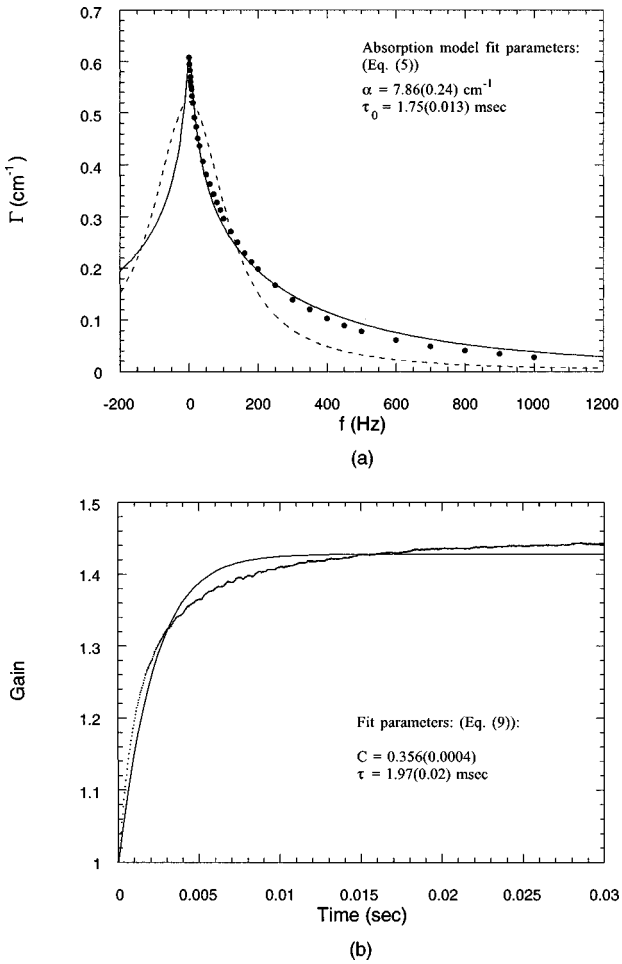

Fig. 8. Temporal response of the GaAs: Cr sample. $1/e^2$ beam diameters, 2.0 mm (pump) and 1.8 mm (signal). Spatially averaged beam intensities are $I_{\text{pump}} = 1.55$ W/cm^2 and $I_{\text{signal}} = 2.4$ mW/cm^2. (a) Frequency response. Solid curve, fit to the absorption model; dashed curve, fit to a Lorentzian. (b) Time response. The curve is a fit to a single-exponential growth model.

The discrepancies between the data in Fig. 8 and the response expected from the simple theory can be attributed to the nonuniform intensity present inside the volume of the crystal occupied by the signal beam. As stated above, the sources of the nonuniformity in our case are the crystal absorption and the Gaussian beam profiles.

As was shown in Section 2, in the case of plane-wave beams the shape of the gain spectrum can be predicted by use of the known absorption coefficient of the material [see Eq. (5)]. However, an attempt to fit the frequency-response data of Fig. 8(a) to Eq. (5) yields a fitted value of the absorption coefficient that differs by a factor of >6 from the actual value of 1.2 cm^{-1}. This result is due to the fact that the absorption model does not account for the Gaussian nature of the pump beam or the experimental geometry. The fit to Eq. (5) is therefore somewhat artificial in the sense that the fitting parameters are not expected to match the actual values that they are meant to represent. Since the effect of non-plane-wave beams is always to reduce the frequency bandwidth, an attempt to fit the frequency-response data to a model that neglects beam profiles always yields an absorption-fitting param-

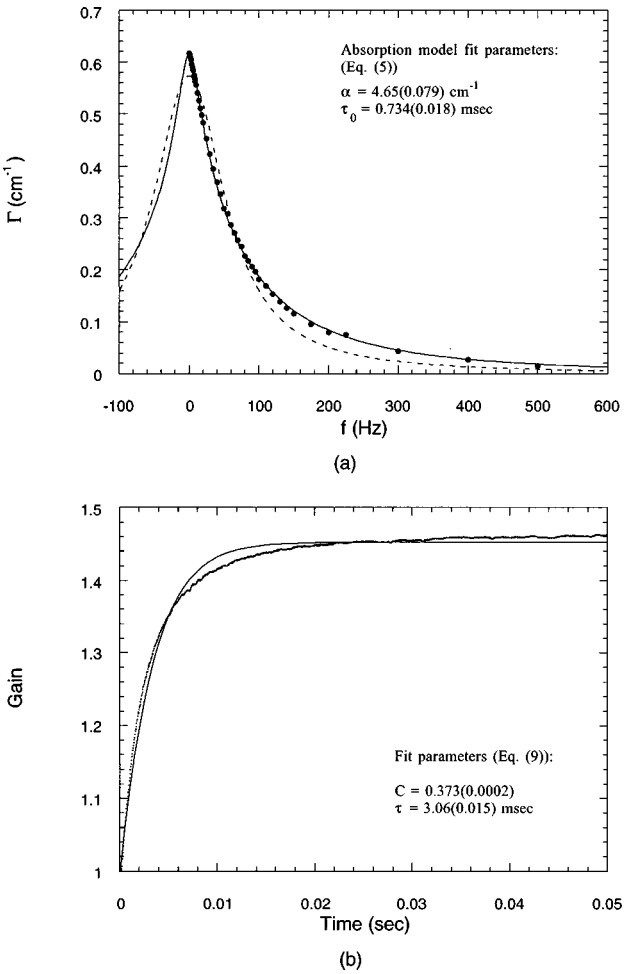

Fig. 9. Temporal response of the GaAs: Cr sample. $1/e^2$ beam diameters, 6.0 mm (pump) and 1.8 mm (signal). Spatially averaged beam intensities are $I_{\text{pump}} = 172$ mW/cm^2 and $I_{\text{signal}} = 2.4$ mW/cm^2. (a) Frequency response. Solid curve, fit to the absorption model; dashed curve, fit to a Lorentzian. (b) Time response. The curve is a fit to a single-exponential growth model.

eter that equals or exceeds the actual absorption coefficient. This result reflects the combined effects of the small Gaussian pump beam, the two-beam coupling geometry (including beam crossing angle and the crossing position of the beams in the crystal), and the crystal thickness.

The solid curve in Fig. 8(b) is a fit of the time-response data to a single exponential rise:

$$\frac{I_{\text{sig}}(z = d/\cos\theta;\ \text{pump on})}{I_{\text{sig}}(z = d/\cos\theta;\ \text{pump off})} = \exp[-\Gamma(t)d/\cos\theta] = \exp\{C[1 - \exp(-t/\tau)]\}, \tag{9}$$

where $I_{\text{sig}}(z = d/\cos\theta;\ \text{pump on})$ is the signal beam intensity with the pump beam present, $I_{\text{sig}}(z = d/\cos\theta;\ \text{pump off})$ is the signal beam intensity with no pump beam, the signal beam is assumed to propagate in the z direction, C is a constant that determines the steady-state gain, d is the crystal thickness, and θ is beam crossing half-angle. Not surprisingly, these data show a correspondingly large deviation from the simple time-response model, and the fit to Eq. (9) yields fitting parameters that do not reflect the actual time response of the system, as it is not single exponential.

The effect on the temporal response of increasing the diameter of the Gaussian pump beam is shown in Figs. 9 and 10, in which the pump beam $1/e^2$ diameters have been increased to 6.0 and 10.7 mm, respectively. The signal beam diameter remains at 1.8 mm. Note that the quality of the fit in Figs. 9(a) and 10(a) to the pure absorption model [solid curves; Eq. (5)] is extremely good, even though the fitted absorption parameters still deviate from the actual value of the absorption coefficient by factors of 3.9 and 2.0, respectively. As expected, the time-domain data in Figs. 9(b) and 10(b) show a deviation from single-exponential response.

In our experiment we had insufficient laser power to simultaneously achieve a plane-wave pump beam and a large pump–signal intensity ratio. These conditions would have allowed us to extract an accurate material time constant from a fit of the frequency-response data to the absorption model. Because of this experimental limitation, we took an alternative approach that consisted of

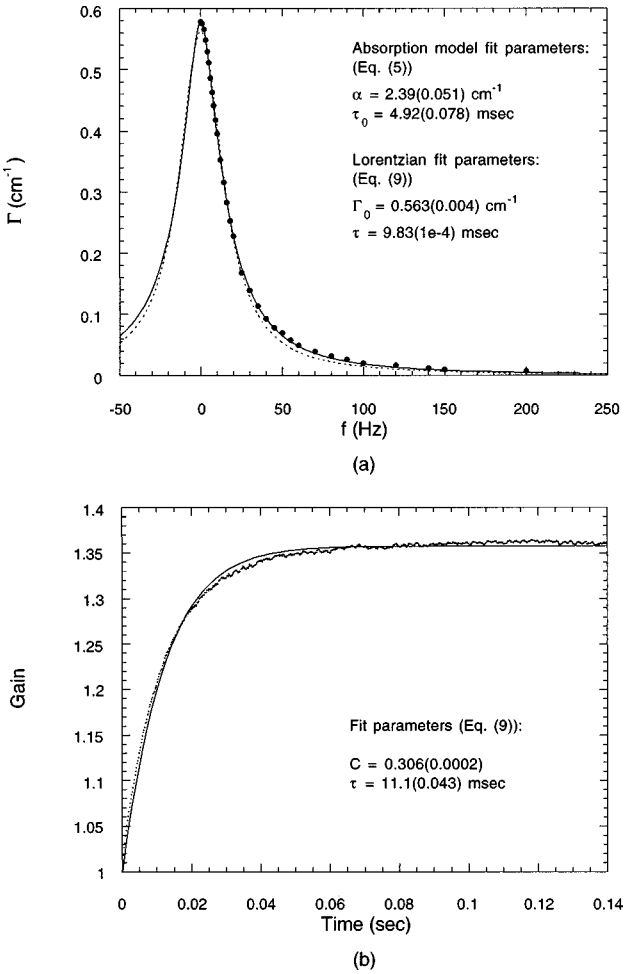

Fig. 10. Temporal response of the GaAs: Cr sample. $1/e^2$ beam diameters, 10.7 mm (pump) and 1.8 mm (signal). Spatially averaged beam intensities are $I_{\text{pump}} = 54$ mW/cm^2 and $I_{\text{signal}} = 2.4$ mW/cm^2. (a) Frequency response. Solid curve fit to the absorption model; dashed curve fit to a Lorentzian. (b) Time response. The curve is a fit to a single-exponential growth model.

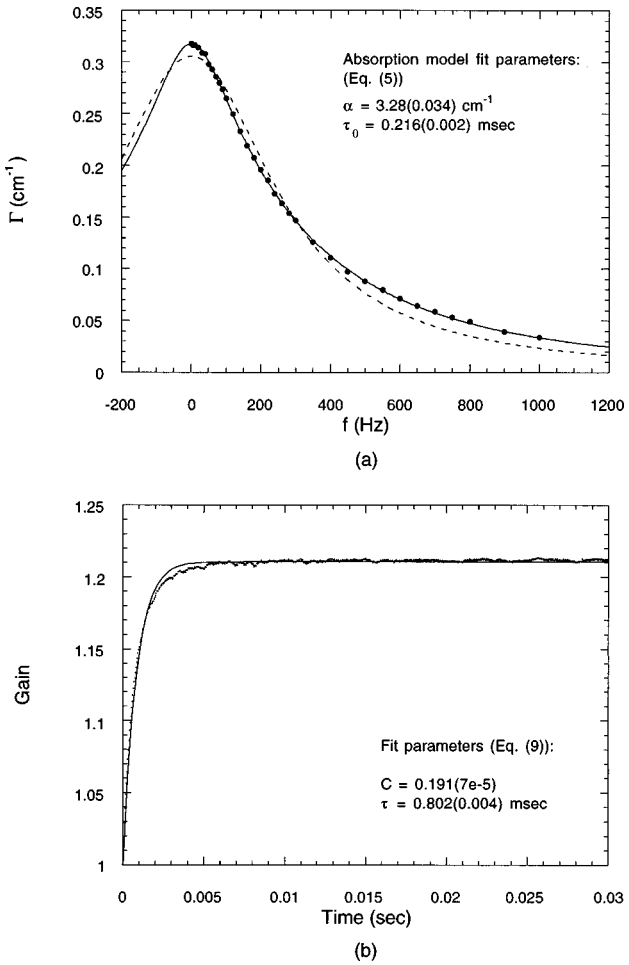

Fig. 11. Temporal response of the GaAs: Cr sample in the presence of a flood beam. $1/e^2$ beam diameters, 2.0 mm (pump), 1.8 mm (signal), and 13.0 mm (flood). Spatially averaged beam intensities are $I_{\text{pump}} = 1.55$ W/cm^2, $I_{\text{signal}} = 2.4$ mW/cm^2, and $I_{\text{flood}} = 142$ mW/cm^2. (a) Frequency response. Solid curve, fit to the absorption model; dashed curve, fit to a Lorentzian. (b) Time response. The curve is a fit to a single-exponential growth model.

illuminating the crystal incoherently from the exit face side with a large-diameter beam at the same wavelength as the pump and the signal beams, obtained from a separate laser. If the intensity and the diameter of this flood beam are chosen appropriately, the effect is to significantly reduce the intensity variations in the crystal that are due to all sources. To the degree that intensity uniformity is accomplished, the frequency response should take on the Lorentzian shape of the zero-absorption, plane-wave theory of Eqs. (1) and (2).

Figures 11–13 show frequency- and time-response data with a flood beam illuminating the crystal from the exit face side. Except for the addition of the floodlight, the conditions for the data of Figs. 11, 12, and 13 were identical to those in Figs. 8, 9, and 10, respectively. If we compare Figs. 11(a) and 8(a), for both of which the pump beam is at its smallest diameter (2.0 mm), we can see that the addition of the floodlight in Fig. 11(a) has caused the frequency response to approach Lorentzian behavior. The remaining discrepancy is due to the fact that the pump beam intensity is more than ten times that of the flood in this case, so the flood beam is unable to completely compensate for the intensity nonuniformity in the crystal. In Fig. 12 the pump and the flood beams are similar in intensity and the pump beam diameter has been increased relative to that in Fig. 11, to 6.0 mm. In this case the frequency-response data come quite close to fitting a Lorentzian function, an indication that the intensity distribution in the crystal is approaching uniformity. This is also apparent in the corresponding time-response data in Fig. 12(b).

The greatest intensity uniformity was achieved with the largest pump beam diameter, 10.7 mm, and with the floodlight illuminating the crystal, with the flood and the pump beam intensities approximately equal. These data are shown in Fig. 13, and from the Lorentzian and single-exponential fits in Fig. 13 come our best estimate of the material time constant for this GaAs sample. The time constants obtained from the frequency- and time-domain data in Fig. 13 are in close, but not perfect, agreement. This difference is due to the small amount of remaining intensity nonuniformity in the crystal, which is evident from the small deviation of the frequency-response data

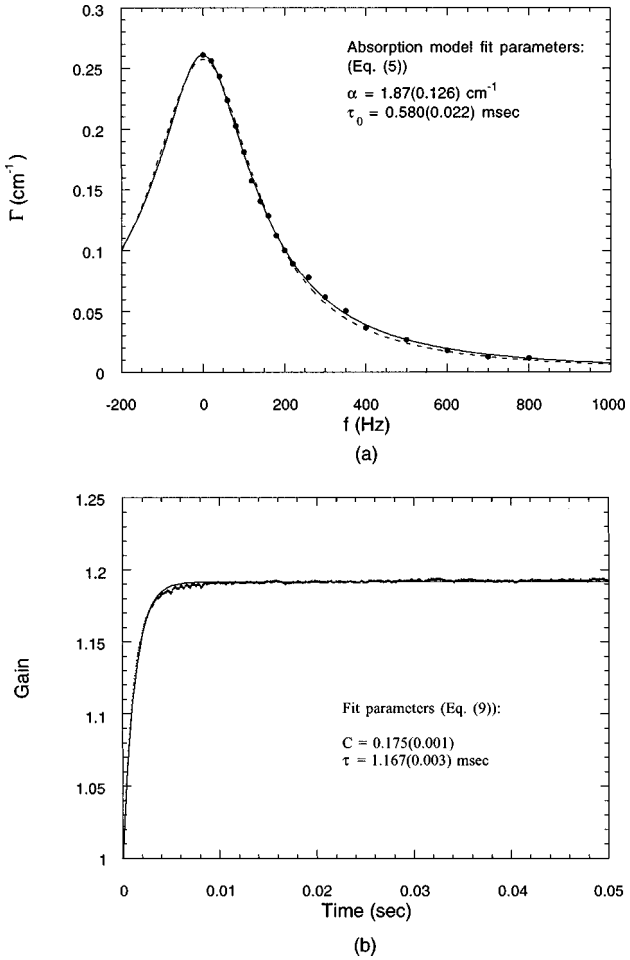

Fig. 12. Temporal response of the GaAS: Cr sample in the presence of a flood beam. $1/e^2$ beam diameters, 6.0 mm (pump), 1.8 mm (signal), and 13.0 mm (flood). Spatially averaged beam intensities are $I_{\text{pump}} = 172$ mW/cm^2, $I_{\text{flood}} = 142$ mW/cm^2. (a) Frequency response. Solid curve, fit to the absorption model; dashed curve, fit to a Lorentzian. (b) Time response. The curve is a fit to a single-exponential growth model.

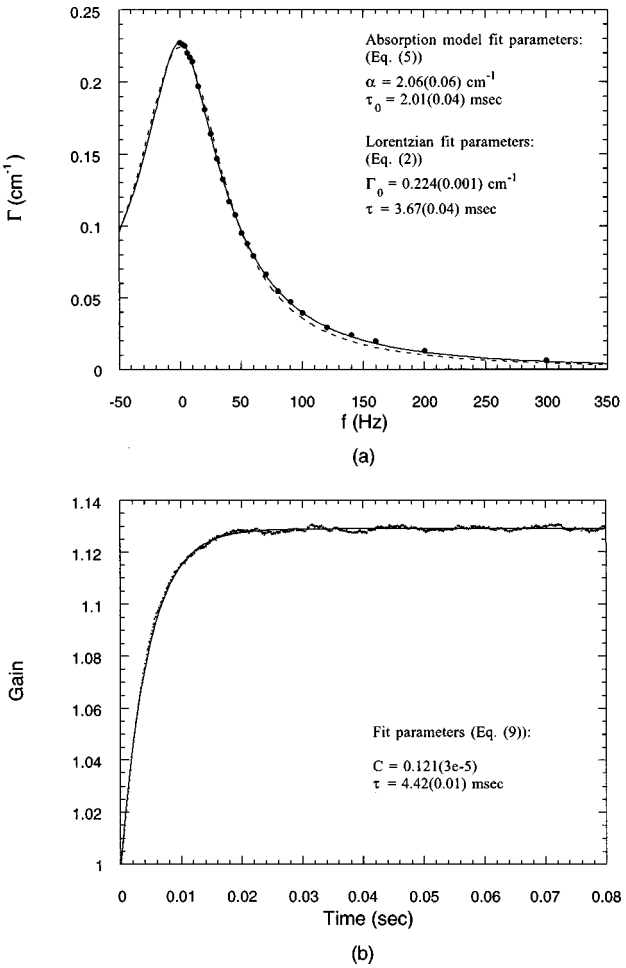

Fig. 13. Temporal response of the GaAs: Cr sample in the presence of a flood beam. $1/e^2$ beam diameters, 10.7 mm (pump) and 1.8 mm (signal). Spatially averaged beam intensities are $I_{\text{pump}} = 54$ mW/cm^2, $I_{\text{signal}} = 2.4$ mW/cm^2 and $I_{\text{flood}} = 48$ mW/cm^2. (a) Frequency response. Solid curve, fit to the absorption model; dashed curve, fit to a Lorentzian. (b) Time response. The curve is a fit to a single-exponential growth model.

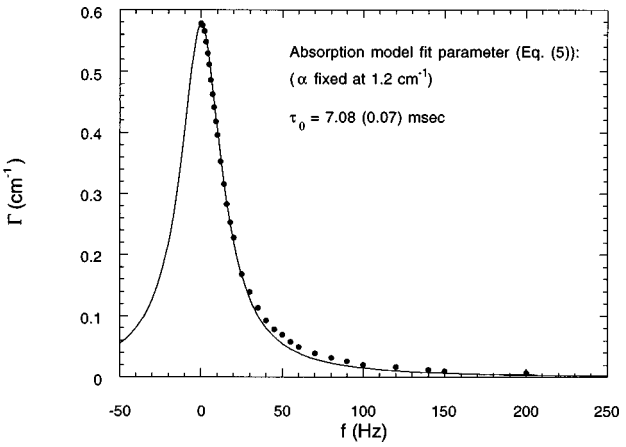

Fig. 14. Fit of the data of Fig. 10(a) to the absorption coefficient parameter held constant at its known value of 1.2 cm^{-1}.

from Lorentzian behavior. Note that it is impossible to completely compensate for material absorption and nonuniform beam profiles by use of a flood beam. However, the goodness of the fits in Fig. 13 and the close agreement of the time constants obtained from the frequency- and time-domain data [3.67 (0.04) ms and 4.42 (0.01) ms, respectively, at an approximate total intensity of 52 mW/cm^2] indicate that a high degree of intensity uniformity has been achieved.

It was mentioned above that the absorption model fit of the frequency-response data in Fig. 10(a), corresponding to the 10.7-mm pump beam and no flood beam, yields an absorption coefficient of 2.4 cm^{-1}, which is twice the actual value. The fitted time constant also differs from the expected value based on the results in Fig. 13 and assuming a linear intensity dependence. Nevertheless, the quality of the fit to the absorption model in Fig. 10(a) is very good. The ability of the absorption model to fit the frequency-response data well in almost all cases while yielding unphysical values of the absorption coefficient and the time constant is due in part to fact that the position-dependent illumination, whether it originates from the absorption or the Gaussian beam profile, decreases the bandwidth. Thus a large absorption coefficient compensates for the beam profile effects. The other factor is the compensating relationship between the two fitting parameters. Increasing (decreasing) the value of the absorption parameter leads to a narrowing (broadening) of the gain bandwidth, and a change in the time constant parameter has the opposite effect. There is, then, a wide range of parameter pairs that yield a reasonable fit to the data. Since the absorption coefficient of the GaAs sample is known, we also fitted the data of Fig. 10(a) to the absorption model with the absorption parameter fixed at its known value of 1.2 cm^{-1}. This fit is shown in Fig. 14, and the resulting fitted time constant is 7.08 (0.07) ms. For comparison, the predicted value of this time constant, based on linear intensity dependence, is 6.8 ms. This is evidence that for this pump beam diameter, 10.7 mm, and for the absence of a flood beam the influence of the Gaussian nature of the pump beam on the photorefractive temporal response has been largely eliminated.

We have observed similar two-beam coupling gain spectrum narrowing effects in four other photorefractive semiconductors: ZnTe:Mn:V, CdMnTe:V, CdTe:Ge, and CdTe:V.

4. CONCLUSIONS

In this paper we have illustrated the influence of bulk absorption, beam profiles, and experimental geometry on measurements of photorefractive temporal response, in the undepleted-pump case and in the limit of small coupling. These effects act to narrow the bandwidth and to cause the spectra to deviate from the expected Lorentzian shape.

We have shown that, if accurate values of the photorefractive material time constant are to be obtained, spatial variations of total laser intensity in the crystal must be either eliminated or accounted for in the model used to extract the temporal parameters. If enough laser power is available, the pump beam can be expanded to closely approximate a plane wave. In this case the absorption model [Eq. (5)] should describe the frequency response, and a fit to this model would yield the material time con-

stant. As we have shown, an alternative method is to achieve an approximately uniform volume intensity distribution by incoherent illumination of the material with a uniform intensity beam. Another method, in principle, is to use a thin sample. However, in addition to depending on the availability of a thin sample that has characteristics similar to the one being used in an actual system, the overall gain in this case may not be sufficient to allow accurate measurements to be made.

ACKNOWLEDGMENTS

Financial support by the European Office of Aerospace Research and Development and by the U.S. Air Force Office of Scientific Research is gratefully acknowledged.

*Present address, Rocketdyne Division, Boeing North American, 6633 Canoga Avenue, P.O. Box 7922, Canoga Park, California 91309.

REFERENCES

1. B. I. Sturman, "Interaction of two light waves in a crystal caused by photoelectron diffusion and drift," Sov. Phys. Tech. Phys. **23**, 589 (1978).
2. P. Yeh, *Introduction to Photorefractive Nonlinear Optics* (Wiley, New York, 1993).
3. L. Dai, C. Gu, and P. Yeh, "Effect of position-dependent time constant on photorefractive two-wave mixing," J. Opt. Soc. Am. B **9**, 1693 (1992).
4. Ph. Delaye, L. A. De Montmorillon, and G. Roosen, "Transmission of time modulated optical signals through an absorbing photorefractive crystal," Opt. Commun. **118**, 154 (1995).
5. A. Hermanns, C. Benkert, D. M. Lininger, and D. A. Anderson, "The transfer function and impulse response of photorefractive two-beam coupling," IEEE J. Quantum Electron. **28**, 750 (1992).
6. D. Fluck, S. Brulisauer, and P. Gunter, "Photorefractive two-wave mixing with focused Gaussian beams," Opt. Commun. **115**, 626 (1995).
7. L. Boutsikaris and F. Davidson, "Two-wave mixing of time-varying non-plane-wave optical fields in photorefractive materials," Appl. Opt. **32**, 1559 (1993).
8. L. Solymar, D. J. Webb, and A. Grunnet-Jepsen, "Forward wave interactions in photorefractive materials," Prog. Quantum Electron. **18**, 377 (1994).
9. F. Vachss, "An analytical expression for the photorefractive two beam coupling response time," presented at the meeting on Photorefractive Materials, Effects, and Devices, cosponsored by the Optical Society of America and Societe Francaise D'Optique, 1990.
10. G. Brost, "Numerical analysis of photorefractive grating formation dynamics at large modulation in BSO," Opt. Commun. **96**, 113 (1993). (Note that the analysis presented here is for an applied field but that for $m = 1$ the results for no applied field are similar.)
11. S. Odoulov, A. Shumelyuk, G. Brost, and K. Magde, "Enhancement of beam coupling in the near infrared for tin hypothiodiphosphate," Appl. Phys. Lett. **69**, 3665 (1996).